Comparison of PIM and RPIM solutions of Elasto-plastic Thick Beams

***B. Kanber[1], N. F. Dogan[1]**

[1]Mechanical Engineering Department, University of Gaziantep, Turkey.

*Corresponding author: kanber@gantep.edu.tr

Abstract

In this study, the point interpolation method (PIM) and radial point interpolation method (RPIM) solutions of elasto-plastic thick beams are compared by using standard Gaussian integration and a nodal integration based on Taylor series expansion. The effects of integration schemes, support domain sizes and RPIM shape parameters on the solution convergence are also investigated after yield point. The global weak form is used to obtain nodal stiffness matrixes. A simply supported beam with constant strength is solved by considering an elasto-plastic hardening material. Its results are compared with finite element solutions in ANSYS.

Keywords: PIM, RPIM, Elasto-plastic, Meshfree, Thick Beams.

Introduction

Beams are mechanical components that are widely used in engineering design. One of the main techniques to analyze beams is the finite element method (FEM) (Owen and Hinton, 1980). Elasto-plastic beams are also analyzed using the finite element method (FEM) (Chebl and Neale, 1984; Lee and McClure, 2005).

Point interpolation method (PIM) is a simple and useful mesh-free technique and originally proposed by Liu and Gu (2001a). In the PIM, the field variables are interpolated using point interpolation shape functions. The main problem in the PIM is the singularity of the moment matrix. The radial point interpolation method (RPIM) is proposed to overcome this problem and based on combining polynomial and radial basis functions (Wang and Liu, 2002a, b; Liu et al., 2005). It becomes a popular technique in the meshfree solution of wide range of problems. It is used in the vibration analysis of 2D solids, shells and beams (Liu and Gu, 2001; Zhao et al., 2009a; Bui et al., 2012), solution of Kirchoff and Mindlin plates (Dinis et al., 2008; Liu et al., 2006; Liew and Chen, 2004; Djeukou and Estorff, 2009), analysis of shell problems (Liu et al., 2006; Zhao et al., 2009b), geometric nonlinear analysis of plates and cylindrical shells (Zhao, 2008), contact analysis of solids (Li et al., 2007), functionally graded materials (Dai et al.,2004) and incompressible flow (Wu and Liu, 2003).

In this study, PIM and RPIM are used to determine the effect of support domain size, RPIM shape parameters and integration schemes on the solution accuracy of elasto-plastic thick beam solutions.

Elasto-Plastic Thick Beams

Under a distributed load intensity q, the beam undergoes a set of virtual lateral displacements δw, virtual normal rotations $\delta\theta$ and associated virtual curvatures $-z[d(\delta\theta)/dx]$ and virtual shear strains $\delta\beta$. Then the global weak form can be expressed as (Owen and Hinton, 1980):

$$\int_0^l \int_{-t/2}^{t/2} \int_{b(-t/2)}^{b(t/2)} \left\{-z\frac{d(\delta\theta)}{dx}\sigma_x + \delta\beta\tau_{xz}\right\} dydzdx - \int_0^l \delta w\, q dx = 0 \quad (1)$$

where t is depth and b is breadth of the beam. Eq. (1) can be expressed as:

$$\left[\boldsymbol{K}_f + \boldsymbol{K}_s\right]\boldsymbol{\varphi} - \boldsymbol{F} = 0 \tag{2}$$

where $\boldsymbol{K}_f$ is the global flexural and $\boldsymbol{K}_s$ is the global shear stiffness matrices. $\boldsymbol{F}$ is the global force vector. Global matrices and vectors can be obtained by assembling their nodal values. In a field node, the nodal stiffness matrices and nodal force vector can be expressed as follows:

$$\begin{aligned} \boldsymbol{k_f} &= \int_{x_1}^{x_2}\left[\boldsymbol{B_f}\right]^T (EI)\boldsymbol{B_f} dx \\ \boldsymbol{k_s} &= \int_{x_1}^{x_2}[\boldsymbol{B_s}]^T (GA)\boldsymbol{B_s} dx \\ \boldsymbol{f} &= \int_{x_1}^{x_2}[\phi_1 \quad 0 \quad \phi_2 \quad 0]^T q\, dx \end{aligned} \tag{3}$$

where x_1 and x_2 are integration borders of an integration domain. In a local support domain (Liu, 2002), if n is considered as number of nodes, the lateral displacement w_i and slope θ_i at a node can be defined in terms of shape functions as follows:

$$\begin{aligned} w_i &= \phi_1 w_1 + \phi_2 w_2 + \cdots + \phi_n w_n \\ \theta_i &= \phi_1 \theta_1 + \phi_2 \theta_2 + \cdots + \phi_n \theta_n \end{aligned} \tag{4}$$

Using the curvature-displacement relationship, $\boldsymbol{B_f}$ can be expressed as:

$$\boldsymbol{B_f} = \left[0 \quad \frac{d\phi_1}{dx} \quad 0 \quad \frac{d\phi_2}{dx} \quad \ldots \quad 0 \quad \frac{d\phi_n}{dx}\right] \tag{5}$$

and $\boldsymbol{B_s}$ is the shear strain-displacement matrix

$$\boldsymbol{B_s} = \left[\frac{d\phi_1}{dx} \quad -\phi_1 \quad \frac{d\phi_2}{dx} \quad -\phi_2 \quad \ldots \quad \frac{d\phi_n}{dx} \quad -\phi_n\right] \tag{6}$$

and *EI* is the *flexural rigidity* and *GA* is the *shear rigidity*, ϕ is the nodal shape function that can be constructed using either PIM or RPIM methods.
Bending moments and shear forces on each support domain can be expressed as (Owen and Hinton, 1980):

$$M = (EI)\boldsymbol{B_f}\boldsymbol{\varphi} = \left(\frac{EI}{l}\right)(\theta_1 - \theta_2) \tag{7}$$

where θ_1 and θ_2 are slopes on the local nodes, l is integration domain length. Shear force varies linearly over support domain, if we evaluate it on the mid-point of domain and assume that it is constant over the domain:

$$Q = (GA)\boldsymbol{B_s}\boldsymbol{\varphi} = (GA)\left\{\left(\frac{w_2 - w_1}{l}\right) - \left(\frac{\theta_1 + \theta_2}{2}\right)\right\} \tag{8}$$

The value of the ultimate moment, in plastic condition can be expressed in terms of yield stress σ_0 as:

$$M_0 = \int_{b(-t/2)}^{b(t/2)} \int_{-t/2}^{t/2} z\, \sigma_0 dz\, dy \tag{9}$$

where $M_0 = \sigma_0(bt^2/4)$ for a rectangular beam. After yielding, flexural rigidity *EI* becomes elasto-plastic flexural rigidity:

$$(EI)_{ep} = EI\left(1 - \frac{EI}{EI+H'}\right) \tag{10}$$

where strain-hardening parameter is $H' = dM/(d\epsilon_f)_p$.

Point Interpolation Method (PIM)

Consider a function $u(x)$ defined in domain Ω, which is represented by field nodes. The $u(x)$ at the point of interest x_Q is approximated in the form as presented by Liu (2010):

$$u(x, x_Q) = \sum_{i=1}^{n} B_i(x) a_i \tag{11}$$

where $B_i(x)$ is the basis function defined in the Cartesian coordinate, a_i is the coefficient for the basis function, *n* is the number of nodes in a local support domain.

When, the polynomial basis function is used as a basis function Eq. (11) can be written as:

$$u(x, x_Q) = \sum_{i=1}^{n} p_i(x) a_i(x_Q) = \boldsymbol{p^T}(x)\, \boldsymbol{a}(x_Q) \tag{12}$$

where $p_i(x)$ is the basis function of monomials, *a* is the coefficient of basis function $p_i(x)$

A polynomial basis in one dimension is:

$$\boldsymbol{p^T}(x) = [1, \mathrm{x}, \mathrm{x}^2, \mathrm{x}^3, \mathrm{x}^4, \ldots, \mathrm{x}^{\mathrm{n}-1}] \tag{13}$$

At node *i*, we have equation in matrix form as:

$$u^{sd} = \boldsymbol{P_Q}\mathbf{a} \tag{14}$$

where generalized displacement vector $\boldsymbol{u}^{sd}$

$$\boldsymbol{u}^{sd} = \{[w_1,\ \theta_1, w_2,\ \theta_2, \ldots, w_n, \theta_n]^T\} \tag{15}$$

and $\boldsymbol{P_Q}$ is the moment matrix for 1D case is given by

$$\boldsymbol{P_Q} = \begin{bmatrix} 1 & x_1 & \ldots & x_1^{n-1} \\ 1 & x_2 & \ldots & x_2^{n-1} \\ \vdots & \vdots & \ddots & \vdots \\ 1 & x_n & \ldots & x_n^{n-1} \end{bmatrix} \tag{16}$$

If the inverse of moment matrix exists, using Eq. (16), we have:

$$\mathbf{a} = \boldsymbol{P_Q^{-1}} \boldsymbol{u}^{sd} \tag{17}$$

Finally, the Eq. (12) becomes:

$$u(x, x_Q) = \sum_{i=1}^{n} p_i(x) a_i(x_Q) = \boldsymbol{p^T P_Q^{-1}} \boldsymbol{u}^{sd} \tag{18}$$

where PIM shape function ϕ:

$$\phi = \boldsymbol{p^T P_Q^{-1}} = [\phi_1(x) \quad \phi_2(x) \ldots \quad \phi_n(x)] \tag{19}$$

Radial Point Interpolation Method (RPIM)

The field variable is approximated using a radial basis function. Thus, equation Eq. (11) becomes:

$$u(x, x_Q) = \sum_{i=1}^{n} B_i(x) a_i = \boldsymbol{R}^T(x)\boldsymbol{a}(x_Q) \tag{20}$$

where $\boldsymbol{a}$ is the unknown constants vector for the radial basis function, $\boldsymbol{R}$ is the radial basis function with $r = x - x_i$. Although $\boldsymbol{R}$ is used itself without powers in the original RPIM, it can be used in the following form to increase its accuracy:

$$\boldsymbol{R}^T = [R_1(r_1)^0, R_2(r_2)^1, R_3(r_3)^2, \dots, R_n(r_n)^{n-1}] \tag{21}$$

In this study, multiquadric radial basis function (MQ RBF) $((r_i^2 + (\alpha_c * d_c)^2)^q)$ is used to construct shape functions. In general form of MQ RBF, it has two shape parameters, α_c and q, which control the shape of functions and their range of values are proposed by Wang and Liu (2002). d_c is the nodal spacing in whole problem domain.

$\mathbf{R}_\mathrm{Q}$ is the moment matrix of RBFs and can be written as follows:

$$\boldsymbol{R_Q} = \begin{bmatrix} R_1(r_1)^0 & R_2(r_1)^1 & \dots & R_n(r_1)^{n-1} \\ R_1(r_2)^0 & R_2(r_2)^1 & \dots & R_n(r_2)^{n-1} \\ \vdots & \vdots & \ddots & \vdots \\ R_1(r_n)^0 & R_2(r_n)^1 & \dots & R_n(r_n)^{n-1} \end{bmatrix} \tag{22}$$

It has an inverse, so vector of coefficients **a** can be calculated as:

$$\mathbf{a} = \boldsymbol{R}_Q^{-1} u^{sd} \tag{23}$$

Substituting Eq. (23) into Eq. (20):

$$u(x, x_Q) = \boldsymbol{R}^T(x)\boldsymbol{R}_Q^{-1} u^{sd} \tag{24}$$

RPIM shape functions $\phi(x)$ are

$$\phi(x) = \boldsymbol{R}^T(x)\boldsymbol{R}_Q^{-1} = [\phi_1(x) \;\; \phi_2(x) \dots \;\; \phi_n(x)] \tag{25}$$

Integration Schemes

Gauss Integration Scheme

To evaluate Eq. (3), two different integration schemes are used. In Gauss integration method, quadrature cells are used to integration. Two sampling points are used to calculate flexural nodal stiffness matrix and one sampling point is used for shear nodal stiffness matrix calculation. Thus,

$$\begin{aligned} \boldsymbol{k_f} &= EI * (Jac) * \left[(w_1)\left([\boldsymbol{B_f}]^{\boldsymbol{T}}_{\boldsymbol{q1}} * [\boldsymbol{B_f}]_{\boldsymbol{q1}} \right) + (w_2)\left([\boldsymbol{B_f}]^{\boldsymbol{T}}_{\boldsymbol{q2}} * [\boldsymbol{B_f}]_{\boldsymbol{q2}} \right) \right] \\ \boldsymbol{k_s} &= GA * (Jac) * \left[(w)\left([\boldsymbol{B_s}]^{\boldsymbol{T}}_{\boldsymbol{q}} * [\boldsymbol{B_s}]_{\boldsymbol{q}} \right) \right] \end{aligned} \tag{26}$$

where *Jac* is the Jacobian, *w, w_1, w_2* are weights, *q, q1, q2* are quadrature points and $\boldsymbol{B_f}$ and $\boldsymbol{B_s}$ are presented in Eq. (5), Eq. (6) respectively.

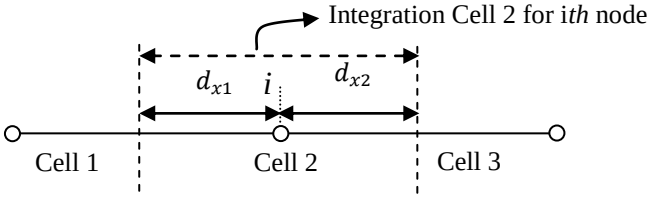

Figure.1 Nodal integration scheme.

4.2 Nodal Integration Scheme

Second integration scheme is the nodal integration proposed by Liu et al. (2007). In this method, nodal stiffness matrices are introduced by Taylor's expansion. The whole solution domain is divided into non-overlapping cells around each field node as shown in Fig. 1. Thus, the nodal stiffness matrices can be expressed as:

$$\boldsymbol{k_f} = EI * \left\{ \begin{array}{c} \left([\boldsymbol{B_f}]^{\boldsymbol{T}}_{\boldsymbol{x_0}} * [\boldsymbol{B_f}]_{\boldsymbol{x_0}}\right)(d_{x2} - d_{x1}) + \frac{1}{2!}.\frac{\partial}{\partial x}\left([\boldsymbol{B_f}]^{\boldsymbol{T}}_{\boldsymbol{x_0}} * [\boldsymbol{B_f}]_{\boldsymbol{x_0}}\right)(d_{x2}^2 - d_{x1}^2) \\ + \frac{1}{3!}\frac{\partial^2}{\partial x^2}\left([\boldsymbol{B_f}]^{\boldsymbol{T}}_{\boldsymbol{x_0}} * [\boldsymbol{B_f}]_{\boldsymbol{x_0}}\right)(d_{x2}^3 - d_{x1}^3) \end{array} \right\}$$

$$\boldsymbol{k_s} = GA * \left\{\left([\boldsymbol{B_s}]^{\boldsymbol{T}}_{\boldsymbol{x_0}} * [\boldsymbol{B_s}]_{\boldsymbol{x_0}}\right)(d_{x2} - d_{x1})\right\} \quad (27)$$

Solutions and Discussions

The programs used in this study are developed in Matlab. A constant strength simply supported beam is used to test the developed programs with an elasto-plastic material of E=200 GPa, $\sigma_y = 50\ MPa$ and $H' = 2 * 10^4$ (Fig. 2). A uniformly distributed load of 110 kN/m is applied with ten different increments. In order to compare solution times of methods, a model with 501 regular distributed nodes is developed and solved. All solutions are carried out using a PC with 2.5 GHz CPU and 4 GByte RAM. Although, it is reported that the computational cost of RPIM is higher than PIM and FEM (Liu, 2002), in this study, it is determined that when standard Gauss integration scheme and non-polynomial augmented RPIM are used, there is no significant difference between them in solution times as shown in Table 1. However, when Nodal integration scheme is used, the solution time is nearly reduced 33%. The elastic displacement distributions are all good agreements for all methods as shown in Fig. 3. The support domain size has no a significant effect on the results of PIM and RPIM as shown in Fig. 4-7. Similarly, α_c has no an important effect in RPIM solutions (Fig. 8 and 9). However, q only gives acceptable results when its value approaches to 1 as shown in Fig. 10 and 11.

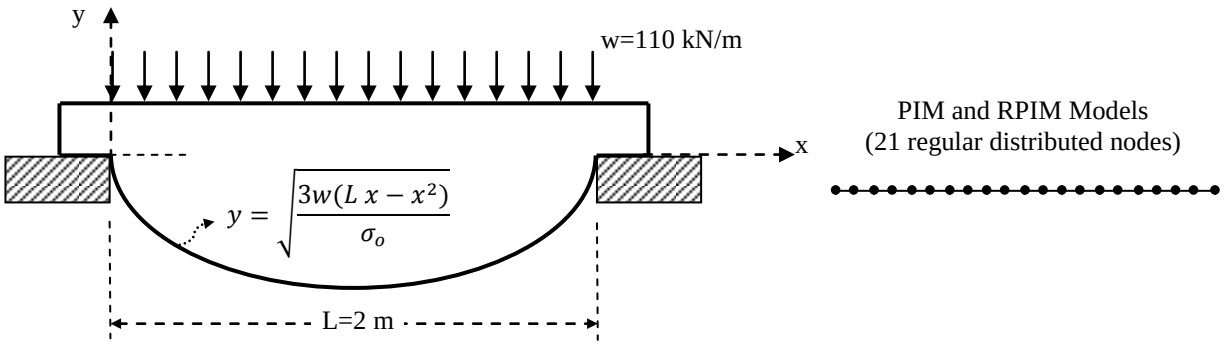

Figure 2.Constant strenght simply supported beam and its PIM and RPIM models.

Table 1. Solution times of Matlab programs for the constant strenght simply supported beam (with 501 regular distributed nodes)

Support Domain Size	Solution times (in Secs)				
	RPIM_Gauss	RPIM_Nodal	PIM_Gauss	PIM_Nodal	FEM
L/10	30.03	20.44	29.96	20.05	29.36
2L/10	30.36	20.61	30.29	20.64	
3L/10	30.41	20.97	30.33	20.98	
4L/10	30.43	21.18	30.38	21.07	
5L/10	30.44	21.52	30.40	21.43	

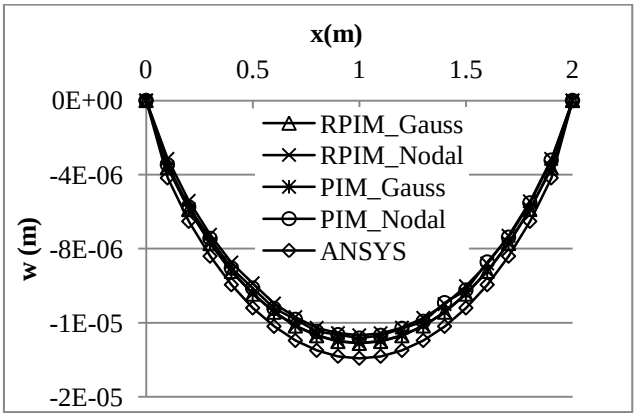

Figure 3. Displacement distribution of constant strength simply supported beam along the neutral axis at the last load increment (w=100 kN/m, sd=L/10 q=1, α_c=3).

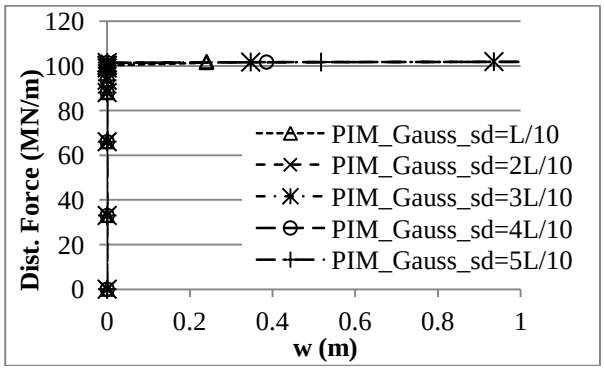

Figure 4. Convergency of the PIM solution of constant strength simply supported beam after yield point for various support domain sizes with q=1, α_c=3 and Gauss integration scheme.

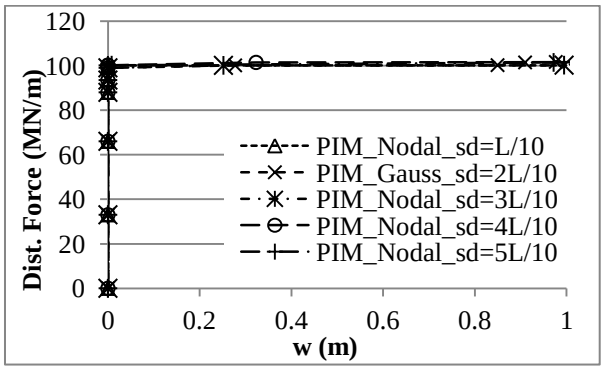

Figure 5. Convergency of the PIM solution of constant strength simply supported beam after yield point for various support domain sizes with q=1, α_c=3 and Nodal integration scheme.

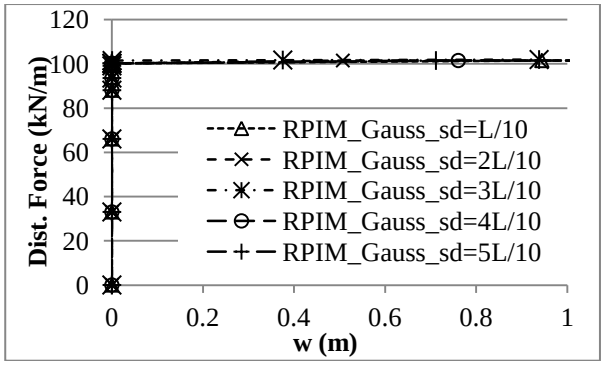

Figure 6. Convergency of the RPIM solution of constant strength simply supported beam after yield point for various support domain sizes with q=1, α_c=3 and Gauss integration scheme.

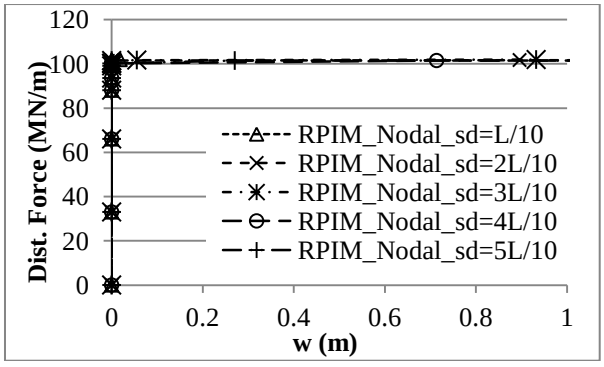

Figure 7. Convergency of the RPIM solution of constant strength simply supported beam after yield point for various support domain sizes with q=1, α_c=3 and Nodal integration scheme.

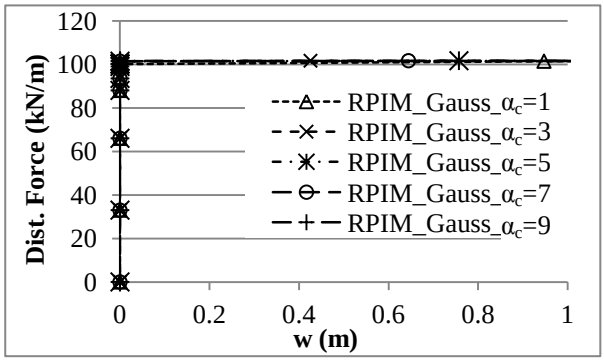

Figure 8. Convergency of the RPIM solution of constant strength simply supported beam after yield point for various α_c with support domain size sd=0.3, q=1 and Gauss integration scheme.

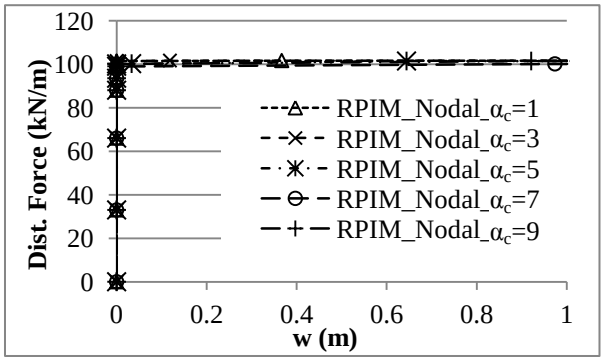

Figure 9. Convergency of the RPIM solution of constant strength simply supported beam after yield point for various α_c with support domain size sd=0.3, q=1 and Nodal integration scheme.

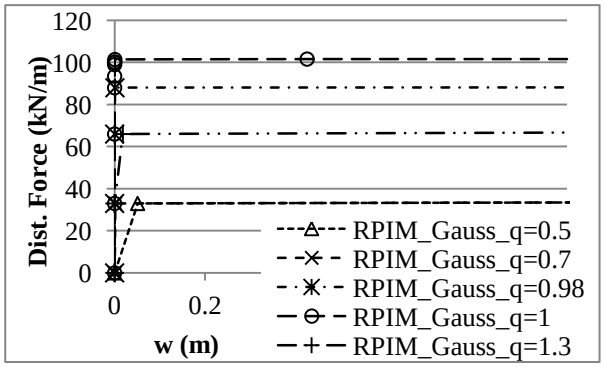

Figure 10. Convergency of the RPIM solution of constant strength simply supported beam after yield point for various q with support domain size sd=0.3, α_c =3 and Gauss integration scheme.

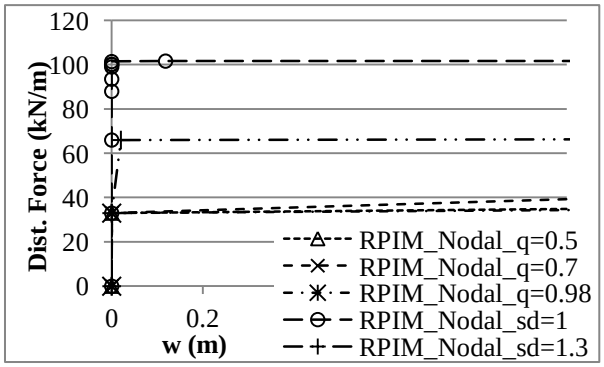

Figure 11. Convergency of the RPIM solution of constant strength simply supported beam after yield point for various q with support domain size sd=0.3, α_c =3 and Nodal integration scheme.

Conclusions

Although in many studies, it is reported that the computational cost of RPIM is higher than FEM and PIM (Liu, 2002), it is shown that solution times of elasto-plastic thick beams are nearly equal to each other's for PIM, RPIM and FEM when standard Gauss integration scheme and non-polynomial augmented RPIM are used. However, when the nodal integration scheme based on Taylor's series expansion is used, the solution times of PIM and RPIM are reduced 33%. The support domain size and α_c do not have a significant effect on the results of all methods. However, q seriously affects the results. It does not give any singular solution when it is equal to 1 and gives best results when it is equal to either 1 or nearly equal to 1.

References

Chebl, C. and Neale K.W. (1984), A finite element method for elasto-plastic beams and colums at large deflections, Computers and Structures, 18, pp.255-261.

Dai, K. Y., Liu, G. R., Lim K. M., Han X. and Du S. Y. (2007), A meshfree radial point interpolation method for analysis of functionally graded material (FGM) plates, Computational Mechanics, 34, 213–223.

Dinis, L.M.J.S., Natal Jorgea, R.M. and Belinha, J. (2008), Analysis of plates and laminates using the natural neighbour radial point interpolation method, Engineering Analysis with Boundary Elements, 32, 267–279.

Gu, Y. T. and Liu, G. R. (2000), A local point interpolation method for static and dynamic analysis of thin beams, Computer Methods in Applied Mechanics and Engineering, 42, pp. 5515-5528.

Lee, P.S. and McClure, G. (2005), A general three-dimensional L-section beam finite element for elasto-plastic large deformation analysis, Computers and Structures, vol.84, pp. 215-229.

Li, Y., Liu, G.R., Luan, M.T., Dai, K.Y., Zhong, Z.H., Li, G.Y. and Han, X. (2007), Contact analysis for solids based on linearly conforming radial point interpolation method, Comput. Mech. 39, 537–554.

Liew, K. M. and Chen, X. L. (2004), Mesh-free radial point interpolation method for the buckling analysis of Mindlin plates subjected to in-plane point loads, Int. J. Numer. Meth. Engng, 60, 1861–1877.

Liu, G. R. (2002): Mesh Free Methods: Moving Beyond the Finite Element Method. CRC press: USA.

Liu, G. R. and Gu, Y. T. (2003), An introduction to Meshfree methods and their programming, Springer: Berlin, 2005.

Liu, G. R. and Gu, Y.T. (2001a), A point interpolation method for two-dimensional solids, Int. J. Numer. Mthds. Engnrg, pp. 937-951.

Liu, G. R. and Gu, Y.T. (2001b), A local radial point interpolation method (LRPIM) for free vibration analyses of 2-d solids, Journal of Sound and Vibration, 246, pp. 29–46.

Liu, G. R., Zhang G. Y., Gu Y. T. and Wang Y. Y. (2005), A meshfree radial point interpolation method (RPIM) for three-dimensional solids, Comput Mech, 36, 421–430.

Liu, G. R., Zhang, G. Y., Wang Y. Y., Zhong, Z. H., Li, G. Y. and Han, X. (2007), A Nodal Integration Technique for Meshfree Radial Point Interpolation Method (NI-RPIM), Journal of Solid and Structures, vol. 44.,pp. 3845-3847.

Liu, L., Chua L.P. and Ghista D.N. (2006), Conforming radial point interpolation method for spatial shell structures on the stress-resultant shell theory, Arch Appl Mech, 75, 248–267.

Liu, Y., Hon Y. C. and Liew K. M. (2006), A meshfree Hermite-type radial point interpolation method for Kirchhoff plate problems, Int. J. Numer. Meth. Engng, 66:1153–1178.

Owen, D.R.J. and Hinton, E. (1980), Finite Elements in Plasticity: Theory and Practice, pp. 121-144

Wang, J. G. and Liu, G. R. (2002a), A point interpolation meshless method based on radial basis functions, Int. J. Numer. Meth. Engng, 54, 1623–1648.

Wang, J. G. and Liu, G. R. (2002b), On the optimal shape parameters of radial basis functions used for 2D meshless methods, Comput. Methods Appl. Mech. Engrg., vol. 191, pp. 2611-2630.

Wu, Y. L. and Liu, G. R. (2004), A meshfree formulation of local radial point interpolation method (LRPIM) for incompressible flow simulation, Computational Mechanics, 30, 355–365.

Zhao, X. , Liu, G. R., Dai K. Y., Zhong Z. H., Li G. Y. and Han X. (2009a), Free-vibration analysis of shells via a linearly conforming radial point interpolation method (LC-RPIM), Finite Elements in Analysis and Design, 45, 917–924.

Zhao, X., Liu, G. R., Dai K. Y., Zhong Z. H., Li G. Y. and Han X. (2009b), A linearly conforming radial point interpolation method (LC-RPIM) for shells, Comput Mech, 43, 403–413.

Zhao, X., Liu, G. R., Dai K. Y., Zhong Z. H., Li G. Y. and Han X. (2008), Geometric nonlinear analysis of plates and cylindrical shells via a linearly conforming radial point interpolation method, Comput Mech, 42, 133–144.